Dyes and Pigments 95 (2012) 322–329

Contents lists available at SciVerse ScienceDirect

Dyes and Pigments

journal homepage: www.elsevier.com/locate/dyepig

Bipolar-transporting dinuclear europium(III) complexes involving carbazole and oxadiazole units: Synthesis, photophysical and electroluminescent properties

Yu Liu*, Jianyu Wang, Yafei Wang, Zhiyong Zhang, Meixiang Zhu, Gangtie Lei, Weiguo Zhu*

Department of Chemistry, Key Lab of Environment-Friendly Chemistry and Application in the Ministry of Education, Xiangtan University, Xiangtan 411105, PR China

ARTICLE INFO

Article history:
Received 12 January 2012
Received in revised form
15 May 2012
Accepted 15 May 2012
Available online 23 May 2012

Keywords:
Dinuclear europium (III) complexes
Bipolar-transporting
Photophysical properties
Electroluminescence
Synthesis
PLEDs

ABSTRACT

A class of bipolar-transporting dinuclear europium (III) complexes involving a carbazole and a oxadizaole fragments was synthesized and characterized by elemental analysis, infrared spectro-scopy and thermal analyses. Compared to the mononuclear europium (III) tris(dibenzoylmethane) (1,10-phenanthroline), these dinuclear europium (III) complexes presented better thermal stability, and similar UV-vis absorption and photoluminescence spectra in dichloromethane. Two intense UV-vis absorption bands at around 282 nm and 352 nm, and a characteris-tical red emission peak at 614 nm from the $^5D_0 \rightarrow {}^7F_2$ transition of the central Eu^{3+} ions were observed under photo-excitation, respectively. Using the $Eu_2(DBM)_6(FPhOXD6CzPhen_2)$ as emitters and a blend of poly (vinylcarbazole) and 2-(4-biphenyl)-5-(4-*tert*-butylphenyl)-1,3,4-oxadiazole as a host matrix, the single emitting-layer polymer light-emitting devices exhibited saturated red electrolumine- scent emission from Eu^{3+} ion at dopant concentrations from 1 wt % to 8 wt %.

1. Introduction

Organic light-emitting diodes (OLEDs) have been intensively studied throughout the world owing to their potential application in the next generation of full-color flat panel displays. For commercial application, three primary colors of blue, green and red are basically required. As europium (III) complexes can emit highly monochromatic red light at around 612 nm with narrow half peak bandwidths of 5–10 nm [1,2] and have a 100% emission quantum efficiency theoretically [3], they have developed to be a class of promising red-emitting materials used in electroluminescent (EL) devices fabricated by vacuum deposition [4–11] and by solution-processing [12–16]. However, compared with the green- and blue-emitting devices, the red-emitting devices using europium complexes as emitters have not yet exhibited satisfying performances although europium complexes presented excellent photoluminescence (PL) properties. In order to improve EL performance of the europium complexes-doped devices, the first way is doping europium (III) complexes into polymers or small molecules with high hole and/or electron mobility [12,17]. The second approach is introducing hole- or electron-transporting units into anionic or ancillary ligands [18–32]. As a result, a wide variety of carrier-transporting groups were introduced into phenanthroline ligand to improve the carrier-transporting properties of their corresponding europium complexes [20–31], in which the hole-transporting groups mainly contain triphenylamine [21,22] and carbazole units [23–27], and the electron-transporting groups mainly are oxadiazole units [28,29]. Both hole- and electron-transporting units sometime were attached into the mononuclear europium (III) complexes [20,30–32]. For example, Zhang et al reported a mononuclear europium (III) complex containing both oxadiazole and triphenylamine units exhibited a high brightness of 1845 cd/m^2 and current efficiency of 2.62 cd/A, as well as a low turn-on voltage of 5.5 V in its OLEDs [31]. Our group successfully achieved a series of bipolar-transporting europium (III) complexes by incorporating both carbazole and oxadiazole units into phenanthroline ligand [32]. These studies showed that these europium (III) complexes bearing both hole- and electron-transporting groups presented improved optophysical and EL properties.

However, all of the mononuclear europium complexes exhibited a concentration quench in their doped devices, which result in lower efficiency and brightness at higher doping concentrations and current density. As dinuclear lanthanide complexes have higher quantum yield than mononuclear lanthanide complexes, study on dinuclear europium complexes has been developed in order to obtain high-efficiency europium complexes-doped OLEDs in recent years [33–38]. For example, Ma group reported a dinuclear europium (III) complex of $(TTA)_3Eu(PYO)_2Eu(TTA)_3$

* Corresponding authors. Tel.: +86 731 58298280; fax: +86 731 58292251.
E-mail addresses: liuyu03b@126.com (Y. Liu), zhuwg18@126.com (W. Zhu).

0143-7208/$ – see front matter © 2012 Elsevier Ltd. All rights reserved.
doi:10.1016/j.dyepig.2012.05.015

(TTA = thenoyltrifluoroacetonate, PYO = pyridine N-oxide), and its doped OLEDs exhibited a brightness of 340 cd/m^2 at a driving voltage of 19 V and a current efficiency of 2.4 cd/A at a current density of 0.14 mA/cm^2, respectively [34]. Gong group reported a dinuclear europium (III) complex of Eu_2(2,7-BTFDBC)$_3$(phen)$_2$ with high thermal stability and intense red emission under blue-light excitation, where 2,7-BTFDBC is 2,7-bis(4'4'4'-trifluoro-1',3'-dioxobutyl) carbazole [37]. Do group reported a dinuclear europium (III) complex of $Eu_2(tta)_6(bpm)_2$ and its doped PVK-PBD (30 wt %) only with a brightness of 30.2 cd/cm^2 at 14 V [38]. To our best knowledge, the bipolar-transporting dinuclear europium (III) complexes incorporated both hole-transporting carbazole and electron-transporting oxadiazole units have not been reported. Moreover, the application of dinuclear europium (III) complexes in OLEDs is rather limited to their photophysical characteristics and thermal stability.

With the same mind, here we designed and synthesized a series of bipolar-transporting dinuclear europium (III) complexes of $Eu_2(DBM)_6$(RPhOXD6CzPhen$_2$) containing a bi-phenanthroline derivatives linked with both hole-transporting carbazole and electron-transporting oxadiazole units. The structure of the $Eu_2(DBM)_6$(RPhOXD6CzPhen$_2$)complexes and their synthetic route are shown in Scheme 1. Their thermal, electrochemical and opto-physical properties were primary investigated. The single-layer polymer light-emitting devices (PLEDs) were fabricated, in which $Eu_2(DBM)_6$(RPhOXD6CzPhen$_2$) is employed as a guest and a blend of poly(N-vinyl-carbazole) (PVK) along with 2-(4-biphenyl)-5-(4-*tert*-butylphenyl)-1,3,4-oxadiaole (PBD) is used as a host matrix. The device electroluminescent performances were studied. A maximum luminance of 48.5 cd/m^2 at 13.3 V was obtained in the device at 4 wt % dopant concentration.

2. Experimental

2.1. Reagents and apparatus

Dibenzoylmethane (HDBM), tetrahydrofuran (THF), N,N-dimethylformamide (DMF), dichloromethane (DCM), ethanol, Eu_2O_3 (99.5%), K_2CO_3 and KOH were analytic reagents and purchased from some reagent companies in China. 4-(5-Aryl-1,3,4-oxadiazole-2-yl)phenol derivatives were prepared according to previous reports [39,40]. 5-Amino-1,10-phenanthroline was prepared according to the literature procedure [41]. The intermediates of RPhOXD6Cz were synthesized according to our previous work [32]. All of the other reagents were used without further purification unless otherwise stated.

All ^{1}H NMR spectra were acquired at a Bruker Dex-400NMR instrument using $CDCl_3$ as solvent. Mass spectra (MS) were recorded on a Bruker Autoflex TOF/TOF (MALDI-TOF) instrument using dithranol as a matrix. Elemental analyses were carried out on

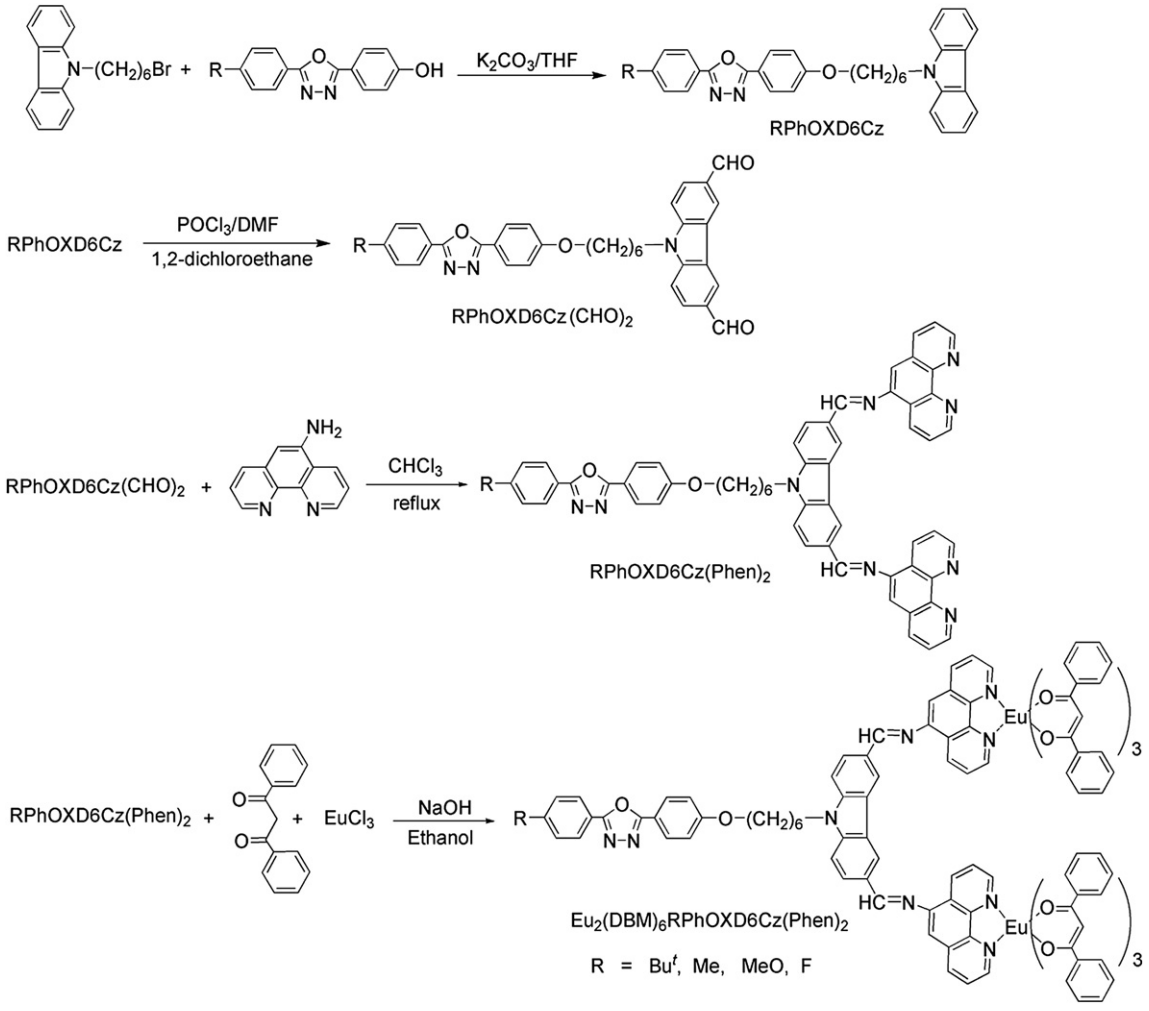

Scheme 1. Synthetic route of the bipolar-transporting dinuclear europium complexes.

a Heraus CHN-rapid elemental analyzer. Thermogravimetric analyses (TGA) were performed under a nitrogen atmosphere at a heating rate of 20 °C/min using a Perkin-Elmer TGA-7 thermal analyzer. The FT-IR spectra were obtained on a Perkin-Elmer spectrum one Fourier transform infrared spectrometer (KBr pellet). Ultraviolet–visible (UV-vis) spectra were measured with a Lambda 25 spectrophotometer. Photoluminescence (PL) spectra were conducted on a Perkin-Elmer LS55 lumine-scent spectrometer with a xenon lamp as a light source. Cyclic voltammetry was carried out on a CHI660A electrochemical workstation in a DCM solution of tetrabutylammonium hexafluorophosphate (Bu_4NPF_6) (0.1 M) with a scan rate of 50 mV/s at room temperature (RT) under nitrogen flow protection.

The single-layer PLEDs with a typical architecture of ITO/PEDOT:PSS (50 nm)/PVK-PBD (30 wt %): europium (III) complex/LiF (0.5 nm)/Al (150 nm) were initially fabricated. The doping concentrations of the europium (III) complex varied from 1 wt %, 2 wt %, 4 wt % to 8 wt %. In the devices, ITO is used as the anode, poly(3,4-ethylenedioxythiophene):poly(styrenesulfonate) (PEDOT:PSS) is used as a hole-injection layer, and LiF/Al is employed as a cathode. The emitting-layer consists of europium (III) complexes and the PVK-PBD blend. The weight ratio of PBD is 30% in the blend.

2.2. Synthesis of ligands and complexes

2.2.1. Synthesis of 9-(6-(4-(5-(4-tert-butylphenyl)-1,3,4-oxadiazol-2-yl)phenoxy)hexyl)-9H-carbazole [Bu^{t}PhOXD6Cz]

2-(4-Hydroxyohenyl)-5-(4-4-tert-butylphenyl)-1,3,4-oxadiazole (2.7 g, 10 mmol), 6-bromo-hexyl-9-H-carbazole (1.8 g, 8.8 mmol), K_2CO_3 (4.4 g, 30.0 mmol), DMF (35 mL) and KI (0.1 g) were stirred at 100 °C for 24 h under nitrogen atmosphere. The resulting mixture was cooled to RT, poured into water (50 mL) and then extracted with DCM (3 × 50 mL). The combined organic layer was dried over anhydrous $MgSO_4$ and filtered. The filtrate was evaporated to remove the solvent and the residue was purified by silica-gel column chromatography using petroleum ether/ethyl acetate (V/V = 5: 1) as eluent to provide a white solid (1.7 g) with a yield of 60%. Mp: 118.0–119.0 °C. ^{1}H NMR(400 MHz, $CDCl_3$, TMS, δ_{ppm}): 8.12–8.10 (d, J = 8.4 Hz, 2H), 8.05–8.03 (m, 4H), 7.55–7.53 (d, J = 8.4 Hz, 2H), 7.46–7.40 (m, 4H), 7.23–7.25 (d, J = 8.4 Hz, 2H), 6.97–6.95 (d, J = 8.5 Hz, 2H), 4.36–4.33 (t, 2H), 4.00–3.96 (t, 2H), 1.98–1.75 (m, 4H), 1.58–1.48 (m, 4H), 1.37 (s, 9H).

2.2.2. Synthesis of 9-(6-(4-(5-(4-methylphenyl)-1,3,4-oxadiazol-2-yl)phenoxy)hexyl)-9H-carbazole [MePhOXD6Cz]

MePhOXD6Cz was prepared according to the synthetic procedure of Bu^{t}PhOXD6Cz. A white solid was obtained with a yield of 58%. Mp: 122.0–123.0 °C. ^{1}H NMR(400 MHz, $CDCl_3$, TMS, δ_{ppm}): 8.12–8.02 (m, 6H), 7.47–7.41 (m, 4H), 7.26–7.23 (d, J = 9.4 Hz, 2H), 7.04–6.95 (m, 4H), 4.59–4.33 (t, 2H), 4.00–3.96 (t, 2H), 2.44 (s, 3H), 1.98–1.75 (m, 4H), 1.58–1.47 (m, 4H).

2.2.3. Synthesis of 9-(6-(4-(5-(4-methoxyphenyl)-1,3,4-oxadiazol-2-yl)phenoxy)hexyl)-9H-carbazole [MeOPhOXD6Cz]

MeOPhOXD6Cz was prepared according to the synthetic procedure of Bu^{t}PhOXD6Cz. A white solid was obtained with a yield of 60%. Mp: 122.0–123.0 °C. ^{1}H NMR(400 MHz, $CDCl_3$, TMS, δ_{ppm}): 8.12–8.02 (m, 6H), 7.47–7.41 (m, 4H), 7.26–7.23 (d, J = 9.4 Hz, 2H), 4.36–4.33 (t, 2H), 4.00–3.96 (t, 2H), 3.89 (s, 3H), 1.98–1.75 (m, 4H), 1.58–1.47 (m, 4H).

2.2.4. Synthesis of 9-(6-(4-(5-(4-fluorophenyl)-1,3,4-oxadiazol-2-yl)phenoxy)hexyl)-9H-carbazole [FPhOXD6Cz]

FPhOXD6Cz was prepared according to the synthetic procedure of Bu^{t}PhOXD6Cz. A white solid was obtained with a yield of 60%. Mp: 125.0–127.0 °C. ^{1}H NMR(400 MHz, $CDCl_3$, TMS, δ_{ppm}): 8.13–8.10 (m, 4H), 8.05–8.03 (d, J = 8.6 Hz, 2H), 7.47–7.43 (m, 4H), 7.25–7.22 (m, 4H), 6.98–6.96 (d, J = 8.4 Hz, 2H), 4.37–4.33 (t, 2H), 4.00–3.97 (t, 2H), 1.96–1.93 (t, 2H), 1.81–1.77 (t, 2H), 1.53–1.47 (m, 4H).

2.2.5. Synthesis of 9-(6-(4-(5-(4-tert-butylphenyl)-1,3,4-oxadiazol-2-yl)phenoxy)hexyl)-9H-carbazole-3,6-dicarbaldehyde [Bu^{t}PhOXD6Cz(CHO)$_2$]

Phosphoryl chloride (4.39 g, 29.0 mmol) was added dropwise to a mixture of DMF (3.8 mL) and 1,2-dichloroethane (3.0 mL) at 0 °C. Bu^{t}PhOXD6Cz (0.76 g, 1.4 mmol) was then added under a vigorously stirring and the resulting mixture was reacted for 48 h at 90 °C. After cooled to RT, the mixture was poured into distilled water (50 mL) and extracted with chloroform (3 × 50 mL). The combined organic layer was dried over anhydrous $MgSO_4$ and filtered. The filtrate was distilled under reduced pressure to remove the solvent, and the residue was purified by silica-gel column chromatography using DCM/ethyl acetate (V/V = 15:1) as eluent to provide a yellow powder (0.37 g) with a yield of 45%. Mp: 128–130 °C. ^{1}H NMR (400 MHz, $CDCl_3$), δ (ppm): 10.13 (s, 2H), 8.67 (s, 2H), 8.10–8.03 (m, 6H), 7.57–7.55 (t, J = 4.2 Hz, 4H), 6.97–6.95 (d, J = 8.0 Hz, 2H), 4.44–4.41 (t, J = 6.4 Hz, 2H), 3.99–3.98 (t, J = 3.2 Hz, 2H), 2.04–1.96 (m, 4H), 1.81–1.77 (m, 4H), 1.37 (s, 9H).

2.2.6. Synthesis of 9-(6-(4-(5-p-tolyl-1,3,4-oxadiazol-2-yl) phenoxy)hexyl)-9H-carbazole-3,6-dicarbaldehyde [CH$_3$PhOXD6Cz(CHO)$_2$]

CH_3PhOXD6Cz(CHO)$_2$ was prepared according to the synthetic procedure of Bu^{t}PhOXD6Cz(CHO)$_2$. A yellow solid was obtained with a yield of 43%. Mp: 129–130 °C. ^{1}H NMR (400 MHz, $CDCl_3$), δ (ppm): 10.14 (s, 2H), 8.68 (s, 2H), 8.11–8.00 (m, 6H), 7.58–7.56 (d, J = 8.2 Hz, 2H), 7.34–7.32 (d, J = 8.0 Hz, 2H) 6.99–6.97 (d, J = 8.8 Hz, 2H), 4.45–4.31 (t, J = 8.4 Hz, 2H), 4.01–3.98 (t, J = 6.2 Hz, 2H), 2.44 (s, 3H), 2.00–1.78 (m, 4H), 1.60–1.49 (m, 4H).

2.2.7. Synthesis of 9-(6-(4-(5-(4-methoxyphenyl)-1,3,4-oxadiazol-2-yl)phenoxy)hexyl)-9H-carbazole-3,6-dicarbaldehyde [MeOPhOXD6Cz(CHO)$_2$]

MeOPhOXD6Cz(CHO)$_2$ was prepared according to the synthetic procedure of Bu^{t}PhOXD6Cz(CHO)$_2$. A yellow solid was obtained with a yield of 42%. Mp: 131–132 °C. ^{1}H NMR(400 MHz, $CDCl_3$), δ (ppm): 10.14 (s, 2H), 8.68 (s, 2H), 8.11–8.02 (m, 6H), 7.58–7.56 (d, J = 8.4 Hz, 2H), 7.04–7.02 (d, J = 8.8 Hz, 2H), 6.97–6.95 (d, J = 8.4 Hz, 2H), 4.45–4.41 (t, J = 8.6 Hz, 2H), 4.01–3.98 (t, J = 6.6 Hz, 2H), 3.89 (s, 3H), 2.05–1.78 (m, 4H), 1.82–1.75 (m, 4H), 1.61–1.49 (m, 4H).

2.2.8. Synthesis of 9-(6-(4-(5-(4-fluorophenyl)-1,3,4-oxadiazol-2-yl)phenoxy)hexyl)-9H-carbazole-3,6-dicarbaldehyde [FPhOXD6Cz(CHO)$_2$]

FPhOXD6Cz(CHO)$_2$ was prepared according to the synthetic procedure of Bu^{t}PhOXD6Cz(CHO)$_2$. A yellow solid was obtained with a yield of 44%. Mp: 127–128 °C. ^{1}H NMR (400 MHz, $CDCl_3$), δ (ppm): 10.16 (s, 2H), 8.70 (s, 2H), 8.15–8.04 (m, 6H), 7.59–7.57 (d, J = 8.4 Hz, 2H), 7.24–7.22 (d, J = 8.4 Hz, 2H), 6.99–6.97 (d, J = 8.4 Hz, 2H), 4.47–4.43 (t, J = 8.2 Hz, 2H), 4.03–4.00 (t, J = 6.2 Hz, 2H), 2.01–1.80 (m, 4H), 1.56–1.49 (m, 4H).

2.2.9. Synthesis of Bu^{t}PhOXD6CzPhen$_2$

Bu^{t}PhOXD6Cz(CHO)$_2$ (0.3 g, 0.5 mmol) dissolved in $CHCl_3$ (20 mL) and a catalytic amount of acetic acid were mixed under stirring for about 20 min 5-amino-1,10-phenanthroline (0.23 g, 1.2 mmol) dissolved in $CHCl_3$ (25 mL) was then added dropwise. The resulting mixture was refluxed for another 24 h under nitrogen protection and distilled to remove excess chloroform under

reduced pressure. Then the mixture was allowed to cool to RT and a yellow solid was formed. The solid was collected and purified by neutral aluminum column chromatography using DCM/ethyl acetate ($V/V = 10:1$) as eluent to give a yellow powder (0.25 g) with a yield of 60%. Mp: 155–156 °C. ^{1}H NMR(400 MHz, $CDCl_3$), δ (ppm): 9.24–9.23 (d, $J = 7$ Hz, 2H), 9.13–9.12 (d, $J = 7$ Hz, 2H), 8.88 (s, 4H), 8.29–8.24 (t, $J = 9.6$ Hz, 4H), 8.06–7.99 (q, 4H), 7.70–7.61 (m, 6H), 7.51–7.49 (d, $J = 8.6$ Hz, 4H), 7.38 (s, 2H), 6.98–6.96 (d, $J = 8.2$ Hz, 2H), 4.51–4.48 (t, $J = 6.4$ Hz, 2H), 4.03–4.00 (t, $J = 6.2$ Hz, 2H), 2.08–2.02 (m, 2H), 1.85–1.81 (t, $J = 8.4$ Hz, 2H), 1.35 (s, 9H), 1.25–1.20 (m,4H). TOF-MS: 954.

2.2.10. Synthesis of CH_3PhOXD6CzPhen$_2$

CH_3PhOXD6CzPhen$_2$ was prepared according to the synthetic procedure of Bu^{t}PhOXD6CzPhen$_2$. A yellow solid was obtained with a yield of 56%. Mp: 157–159 °C. ^{1}H NMR (400 MHz, $CDCl_3$), δ (ppm): 9.25–9.23 (d, $J = 7.0$ Hz, 2H), 9.15–9.14 (d, $J = 7.2$ Hz, 2H), 8.89 (s, 4H), 8.32–8.26 (t, $J = 10.2$ Hz, 4H), 8.10–7.94 (m, 4H), 7.70–7.61 (m, 6H), 7.51–7.49 (d, $J = 8.6$ Hz, 4H), 7.39 (s, 2H), 6.98–6.96 (d, $J = 8$ Hz, 2H), 4.51–4.48 (t, $J = 6.4$ Hz, 2H), 4.03–4.00 (t, $J = 6.6$ Hz, 2H), 2.08–2.02 (m, 2H), 1.85–1.81 (t, $J = 8.2$ Hz, 2H), 1.35(s, 3H), 1.25–1.20 (m, 4H). TOF-MS: 912.

2.2.11. Synthesis of MeOPhOXD6CzPhen$_2$

MeOPhOXD6CzPhen$_2$ was prepared according to the synthetic procedure of Bu^{t}PhOXD6CzPhen$_2$. A yellow solid was obtained with a yield of 50%. Mp: 158–159 °C. ^{1}H NMR(400 MHz, $CDCl_3$), δ (ppm): 9.26–9.25 (d, $J = 2.4$ Hz, 2H), 9.15–9.14 (d, $J = 2.4$ Hz, 2H), 8.89 (s, 4H), 8.30–8.26 (t, $J = 8.6$ Hz, 4H), 8.06–7.99 (m, 6H), 7.72–7.62 (m, 6H), 7.39 (s, 2H), 6.98–6.96 (t, $J = 4.2$ Hz, 4H), 4.53–4.49 (t, $J = 8.8$ Hz, 2H), 4.04–4.02 (t, $J = 4.6$ Hz, 2H), 3.88 (s, 3H), 2.09–1.83 (m, 8H). TOF-MS: 928.

2.2.12. Synthesis of FPhOXD6CzPhen$_2$

FPhOXD6CzPhen$_2$ was prepared according to the synthetic procedure of Bu^{t}PhOXD6CzPhen$_2$. A yellow solid was obtained with a yield of 58%. Mp: 154–156 °C. ^{1}H NMR(400 MHz, $CDCl_3$), δ (ppm): 9.27–9.26 (d, $J = 2.8$ Hz, 2H), 9.16–9.15 (d, $J = 2.8$ Hz, 2H), 8.90 (s, 4H), 8.31–8.26 (t, $J = 9.6$ Hz, 4H), 8.12–8.05 (m, 4H), 7.72–7.69 (m, 4H), 7.65–7.63 (t, $J = 4.2$ Hz, 4H), 7.40 (s, 2H), 7.24–7.17 (t, $J = 12.6$ Hz, 2H), 6.99–6.98 (d, $J = 7.2$ Hz, 2H), 4.51–4.48 (t, $J = 6.6$ Hz, 2H), 4.52–4.48 (t, $J = 8.2$ Hz, 2H), 4.05–4.02 (t, $J = 6.6$ Hz, 2H), 2.09–1.82 (m, 8H). TOF-MS: 916.

2.2.13. Synthesis of Eu$_2$(DBM)$_6$(Bu^{t}PhOXD6CzPhen$_2$)

Eu_2O_3 (0.037 g, 0.12 mmol) was dissolved in concentrated hydrochloric acid (1 mL) at 80 °C and formed white $EuCl_3 \cdot 6H_2O$. This europium chloride was cooled to RT and further dissolved in ethanol (3.0 mL) for the following procedure. After a solution of HDBM (0.161 g, 0.72 mmol) in 6 mL ethanol was neutralized to pH = 6.5–7 with 1 mol/L NaOH aqueous solution in a 25 mL three-necked flask under stirring, the above europium chloride solution was added dropwise into the HDBM solution. The reaction mixture was stirred for 30 min under RT and a solution of Bu^{t}PhOXD6CzPhen$_2$ (0.1 g, 0.1 mmol) in THF (2.0 mL) was added. The resulting mixture was then carefully adjusted to pH = 6.5–7 again with 1 mol/L NaOH aqueous solution and continued to be stirred for 12 h at 50 °C. After cooled to RT, the mixture was added dropwise into 25 mL ethanol to form precipitate. The precipitate was collected and washed with water and ethanol alternately, further purified by recrystallization with a mixing solvent (THF and ethanol, $V/V = 1:5$) to provide a yellow solid (0.17 g) with a yield of 65.0%. Mp: 174–175 °C. FT-IR (KBr, cm^{-1}) 2926, 2342, 1610, 1595, 1550, 1517, 1478, 1458, 1411, 1308, 1220, 1176, 1068, 1024, 838, 810, 737, 723, 690, 521, 436. Anal. calcd. for $Eu_2C_{152}H_{123}N_9O_{14}$ (2603.58): C, 70.12; H, 4.76; N, 4.84. Found: C, 70.62; H, 4.95; N, 5.12.

2.2.14. Synthesis of Eu$_2$(DBM)$_6$(MePhOXD6CzPhen$_2$)

Eu$_2$(DBM)$_6$(MePhOXD6CzPhen$_2$) was prepared according to the synthetic procedure of Eu$_2$(DBM)$_6$(Bu^{t}PhOXD6CzPhen$_2$). A yellow solid was obtained with a yield of 60.0%. Mp: 175–176 °C. FT-IR (KBr, cm^{-1}) 2927, 2345, 1611, 1595, 1550, 1518, 1478, 1458, 1412, 1309, 1256, 1220, 1177, 1068, 815, 738, 724, 521, 434. Anal. calcd. for $Eu_2C_{149}H_{117}N_9O_{14}$ (2561.5) : C, 69.87; H, 4.60; N, 4.92. Found: C, 69.60; H, 4.34; N, 4.85.

2.2.15. Synthesis of Eu$_2$(DBM)$_6$(MeOPhOXD6CzPhen$_2$)

Eu$_2$(DBM)$_6$(MeOPhOXD6CzPhen$_2$) was prepared according to the synthetic procedure of Eu$_2$(DBM)$_6$(Bu^{t}PhOXD6CzPhen$_2$). A yellow solid was obtained with a yield of 58%. Mp: 178–179 °C. FT-IR (KBr, cm^{-1}) 2930, 2344, 1610,1595, 1550, 1517, 1494, 1478, 1458, 1411, 1308, 1220, 1173, 1068, 1025, 839, 811, 723, 609, 519, 435. Anal. calcd. for $Eu_2C_{149}H_{117}N_9O_{15}$ (2577.5): C, 69.43; H, 4.58; N, 4.89. Found: C, 70.02; H, 4.71; N, 4.85.

2.2.16. Synthesis of Eu$_2$(DBM)$_6$(FPhOXD6CzPhen$_2$)

Eu$_2$(DBM)$_6$(FPhOXD6CzPhen$_2$) was prepared according to the synthetic procedure of Eu$_2$(DBM)$_6$(Bu^{t}PhOXD6CzPhen$_2$). A yellow solid was obtained with a yield of 62.0%. Mp: 174–176 °C. FT-IR (KBr, cm^{-1}) 2927, 2343, 1611, 1595, 1550, 1518, 1494, 1478, 1458, 1412, 1310, 1176, 1068, 811, 745, 723, 520, 436. Anal. calcd. for $Eu_2C_{148}H_{114}FN_9O_{14}$ (2565.47): C, 69.29; H, 4.48; N, 4.91. Found: C, 69.52; H, 4.34; N, 4.86.

3. Results and discussion

3.1. IR absorption spectrum

These bipolar-transporting dinuclear europium complexes displayed similar IR spectra in Fig. 1. Three stretching vibration peaks from the C=O, C=C and C=N double bands, company -ing with a bending vibration in plane from the C–H bond, are observed at 1595 cm^{-1}, 1518 cm^{-1}, 1610 cm^{-1} and 1410 cm^{-1}, respectively. It indicates that β-diketone ligand of HDBM is coordinated to Eu^{3+} ion. The strong bending vibration peaks out of plane from the C–H bonds in phenanthroline ring are displayed at 811 and 723 cm^{-1}.

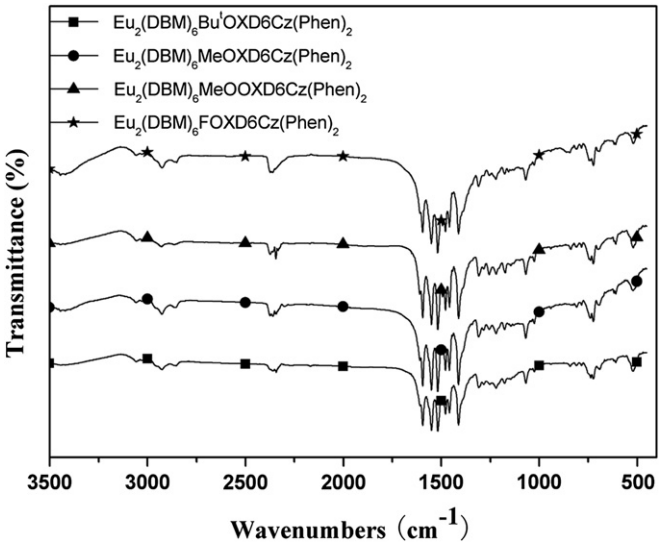

Fig. 1. Infrared spectra of europium complexes.

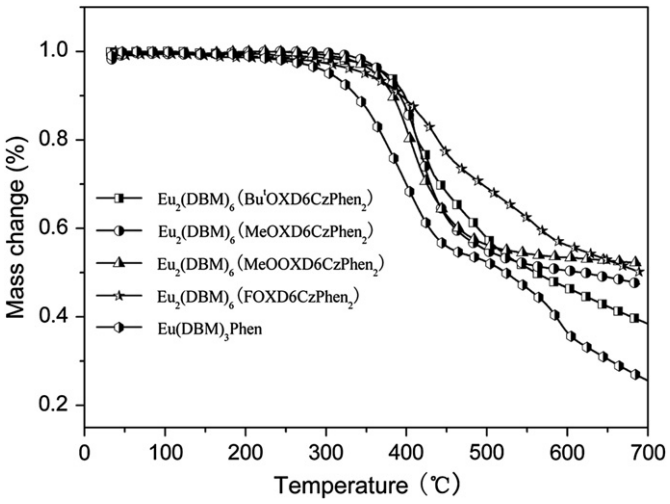

Fig. 2. TG curves of europium complexes recorded in dynamic nitrogen atmosphere (50 mL/min) and heating rate of 20 °C/min.

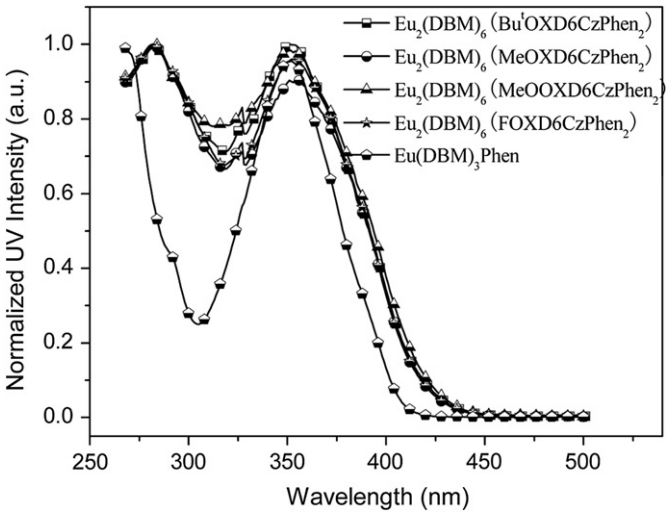

Fig. 3. Normalized UV-vis absorption spectra of europium complexes in dichloromethane solution (1.0×10^{-5} mol/L).

The additional new weak vibration bands at 520 and 435 cm^{-1} are ascribed to Eu-N and Eu-O vibrations, respectively. It further means that the phenanthroline derivatives of $RPhOXD6CzPhen_2$ were together coordinated to Eu^{3+} ion [42]. The IR data of these europium (III) complexes were according with those of the other europium (III) complexes reported in the previous reference [43]. Therefore, the $Eu_2(DBM)_6(RPhOXD6CzPhen_2)$ were confirmed to be formed by the IR data.

3.2. Thermal stability

The thermal properties of europium complexes were determined by thermogravimetric (TG) analysis under N_2 stream with a scanning rate of 20 °C/min and their TG curves are shown in Fig. 2. All these bipolar-transporting dinuclear europium complexes of $Eu_2(DBM)_6(RPhOXD6CzPhen_2)$ exhibited high thermal stability. Their decomposition temperature (T_d) values varied from 349.0 °C to 374.0 °C, which corresponds to a 5% weight loss (Table 1). Compared to the known europium (III) tris(dibenzoylmethane)(1,10-phenanthroline) [$Eu(DBM)_3Phen$] (T_d = 297.0 °C), these dinuclear europium complexes exhibited better thermal stability. It implies that incorporating a bi-phenanthroline derivative of $RPhOXD6CzPhen_2$ with both carbazole and oxadiazole units into europium complex is favorable to enhance its thermal stability. Furthermore, the substituent groups in the oxadiazole unit have a different effect on the thermal stability. An electron-donoring substituent is more efficient to improve the thermal stability of its europium complexes.

3.3. UV absorption property

The normalized UV-vis absorption spectra of the bipolar-transporting dinuclear complexes of $Eu_2(DBM)_6(RPhOXD6CzPhen_2)$ and the mononuclear complex of $Eu(DBM)_3Phen$ in dilute DCM solution (10^{-5} mol L^{-1}) are illustrated in Fig. 3. All the bipolar-transporting dinuclear europium complexes show an intense high-energy absorption band at about 282 nm and a strong low-energy absorption band at about 352 nm, in which the former absorption band is attributed to $\pi-\pi^*$ transition of the bi-phenanthroline derivatives of $RPhOXD6CzPhen_2$ and the latter absorption band is attributed to $\pi-\pi^*$ transition of the DBM anion [28]. Compared to $Eu(DBM)_3Phen$, these bipolar-transporting europium complexes exhibited a similar low-energy absorption band, and a red-shifted high-energy absorption band [14]. This indicates that the incorporated bipolar-transporting units have a significant effect on UV-vis absorption spectra of their europium complexes.

3.4. Photoluminescence property

The normalized PL spectra of europium complexes in DCM at RT are shown in Fig. 4. All these bipolar-transporting dinuclear europium complexes display an intense sharp low-energy emission peak at 614 nm and a broad high-energy emission band between 350 and 500 nm, in which the low-energy emission peak is corresponding to the $^5D_0 \rightarrow {}^7F_2$ transition of Eu (III) ion, and the high-energy emission band is assigned to excited states of the bi-phenanthroline deriva-

Table 1
Thermal, optophysical and electrochemical properties of europium complexes.

Complexes	UV-vis absorption[a] λ/nm (ε_{max}/$dm^3mol^{-1}cm^{-1}$)	λ_{em}[b] (nm)	T_d (°C)	E_{ox}[c] (V)	E_{red}[d] (V)	E_{HOMO}[e](eV)	E_{LUMO}[f] (eV)	E_g[c] (eV)
$Eu(DBM)_3Phen$	352 (29945)	614	297	1.25	−1.96	−5.63	−2.42	3.21
$Eu_2(DBM)_6(Bu^tPhOXD6CzPhen_2)$	286 (179445), 352 (158196)	424, 614	374	1.93	−1.65	−6.31	−2.73	3.58
$Eu_2(DBM)_6(MePhOXD6CzPhen_2)$	286 (134540), 352 (139426)	421, 614	371	1.91	−1.65	−6.29	−2.73	3.56
$Eu_2(DBM)_6(MeOPhOXD6CzPhen_2)$	286 (130828), 352 (137503)	435, 614	361	2.10	−1.61	−6.84	−2.77	3.71
$Eu_2(DBM)_6(FPhOXD6CzPhen_2)$	286 (128755), 352 (125415)	420, 614	349	2.00	−1.68	−6.38	−2.70	3.68

[a] Measured in CH_2Cl_2 at a concentration of 10^{-5} mol/L at 298 K.
[b] Measured in CH_2Cl_2 at 298 K.
[c] Estimated according to the reduction potential and the UV-vis absorption spectrum.
[d] Calculated using equation: $E_{1/2} = (E_{pa} + E_{pc})/2$.
[e] $E_{HOMO} = -(4.38 + E^{ox}{}_{1/2})$ eV.
[f] $E_{LUMO} = -(4.38 + E^{red}{}_{1/2})$ eV.

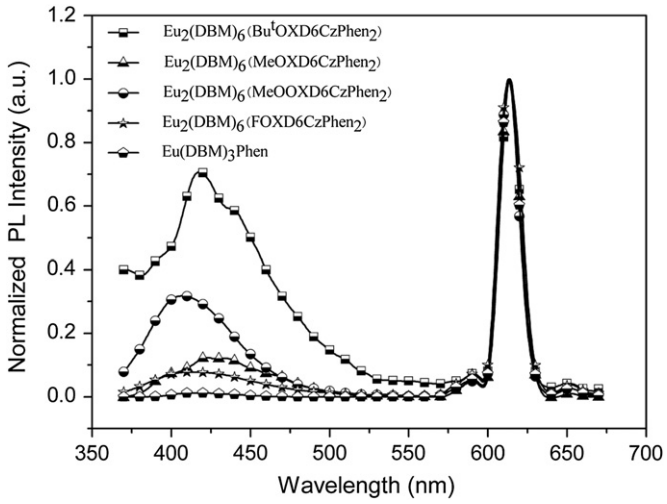

Fig. 4. Normalized photoluminescence spectra of europium complexes in dichloromethane solution (1.0×10^{-5} mol/L, $\lambda_{ex} = 350$ nm).

tives of $RPhOXD6CzPhen_2$ or/and the ligand-to-metal charge transfer (LMCT) transition resulting from the interaction between the central Eu^{3+} ion and the ligand [38]. Compared to $Eu(DBM)_3Phen$, these bipolar-transporting dinuclear europium complexes exhibited an enhanced high-energy emission. Furthermore, the $Eu_2(DBM)_6(Bu^tPhOXD6CzPhen_2)$ and $Eu_2(DBM)_6(FPhOXD6CzPhen_2)$ presented maximum and minimum high-energy emission band in DCM, respectively. Therefore, incorporating an electron-accepting substituent group into oxadiazole unit is available for inhibiting the emission of its bi-phenanthroline derivatives in the europium complexes. In order to further understand the emission property of these bipolar-transporting dinuclear europium (III) complexes, the emission quantum yields were measured using $EuCl_3 \cdot 6H_2O$ ($\Phi_f = 0.073\%$ in water) as standard at RT in DCM based on the literatures [44]. The measured emission quantum yield values of $Eu(DBM)_3Phen$, $Eu_2(DBM)_6(Bu^tPhOXD6CzPhen_2)$, $Eu_2(DBM)_6(MePhOXD6CzPhen_2)$, $Eu_2(DBM)_6(MeOPhOXD6CzPhen_2)$ and $Eu_2(DBM)_6(FPhOXD6CzPhen_2)$ were 0.78%, 10.3%, 10.1%, 9.5% and 10.5%, respectively. It is obvious that these dinuclear europium complexes exhibited twelvefold higher emission quantum yields than the mononuclear $Eu(DBM)_3Phen$ complexes. Among these dinuclear europium complexes, the $Eu_2(DBM)_6(FPhOXD6CzPhen_2)$ presented the highest quantum yield. This indicates that the bi-phenanthroline derivatives bridged with a bipolar-transporting unit can enhance emission quantum yield of their europium complexes [45]. Especially, attaching an electron-accepting fluorine substituent into the oxadiazole unit is more available to improve emission efficiency of its bipolar-transporting dinuclear europium complex.

3.5. Electrochemical property

Cyclic voltammetry (CV) experiments were conducted to detect the electrochemical properties of the europium complexes. All measurements were carried out at RT in a nitrogen-saturated DCM solution of tetrabutylammonium hexafluorophosphate (Bu_4NPF_6, 0.1 M) at a scan rate of 50 mV/s. A platinum rod and a platinum wire were used as the working and counter electrode, respectively. A calomel electrode was used as the reference electrode. Ferrocene was employed as a reference of redox system. The measured concentration of europium complexes was about 2×10^{-4} M. A quasi-reversible reduction wave was observed for these dinuclear europium complexes. The reduction and the oxidation peaks occurred at around −1.55 V and 2.0 V, respectively. The higher oxidation peaks were observed in these dinuclear europium complexes rather than the mononuclear $Eu(DBM)_3Phen$. It means that these dinuclear europium complexes containing bipolar-transporting units are more difficult to be oxidized than the mononuclear europium complex. The highest occupied molecular orbital (HOMO) and the lowest unoccupied molecular orbital (LUMO) energy levels (E_{HOMO} and E_{LUMO}) are calculated according to the following empirical formula: $E_{HOMO} = -e(E_{ox}+4.38)$ and $E_{LUMO} = -e(E_{red}+4.38)$, proposed by Brédas group [46]. The received electrochemical data of europium complexes are listed in Table 1. The HOMO and LUMO energy levels of these bipolar-transporting complexes are −6.29 to −6.48 eV and −2.70 to −2.77 eV, respectively. Compared to the $Eu(DBM)_3Phen$, these dinuclear complexes exhibited a significant decreased HOMO and LUMO energy levels. The decreased LUMO energy levels are available to facilitate electrons injection and transportation from cathode to emitters of europium complexes. Therefore, incorporating both hole-transporting carbazole and electron- transporting oxadiazole units into the bi-phenanthroline derivatives can significantly tune electrochemical and carrier-transporting properties of their dinuclear europium complexes.

3.6. Electroluminescent property

To investigate EL property of these dinuclear europium complexes-doped PLEDs, we used the $Eu_2(DBM)_6(FPhOXD6CzPhen_2)$ as emitter and made the single-layer PLEDs with a configuration of ITO/PEDOT:PSS (50 nm)/PVK-PBD:europium(III) complex/LiF (0.5 nm)/Al (150 nm) because $Eu_2(DBM)_6(FPhOXD6CzPhen_2)$ has the highest PL quantum yield. The normalized EL spectra of the $Eu_2(DBM)_6(FPhOXD6CzPhen_2)$-doped PVK-PBD devices are shown in Fig. 5 with different doping concentrations from 1 wt % to 8 wt % at voltage of 13 V. Extremely sharp red emission centered at around 616 nm is observed for these devices, which is attributed to the europium (III) ion's characteristic emission. At the same time, a minor high-lying emission band around 400–480 nm is also observed at doping concentrations of 1 wt % and 2 wt %, but almost disappear at doping concentrations of 4 wt % and 8 wt %. This high-lying emission is attributed to the emission from exciplex between

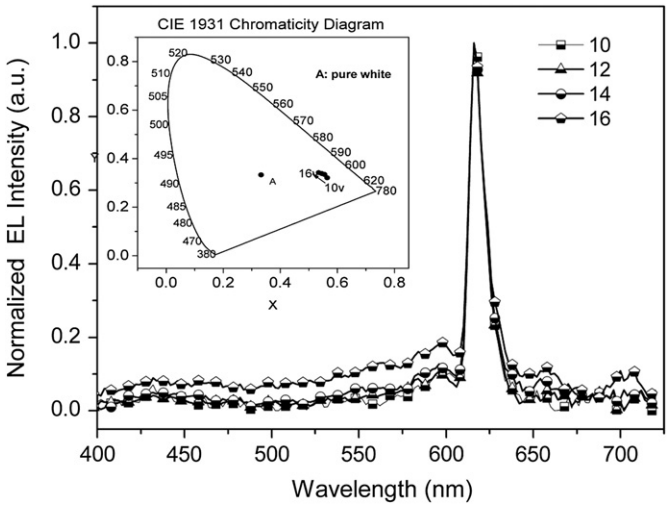

Fig. 5. Normalized EL spectra of the $Eu_2(DBM)_6(FPhOXD6CzPhen_2)$-doped devices at different dopant concentrations from 1 wt % to 8 wt %. Inset: CIE 1931 chromaticity diagrams of these corresponding devices.

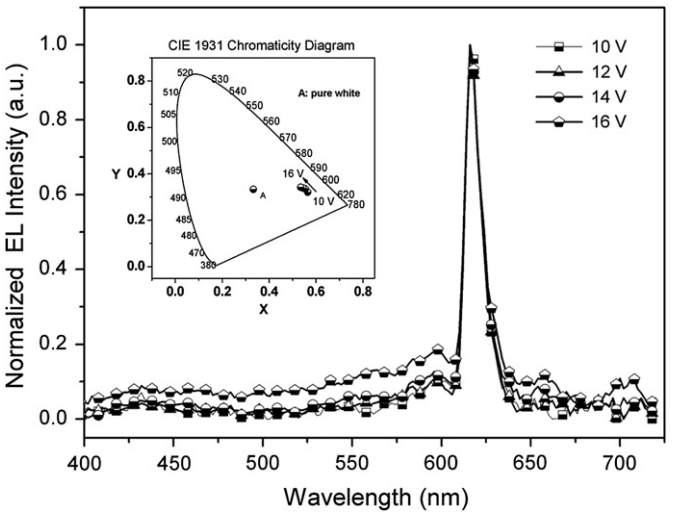

Fig. 6. Normalized EL spectra of the $Eu_2(DBM)_6(FPhOXD6CzPhen_2)$-doped device at 2 wt % dopant concentration under different bias. Inset: CIE 1931 chromaticity diagrams of the corresponding device.

$Eu_2(DBM)_6(FPhOXD6CzPhen_2)$ and PVK [29]. The inset Fig. 5 shows the CIE coordinates diagram for these devices at doping concentrations from 1 wt % to 8 wt %. Significantly different CIE coordinate is displayed with increasing the doping concentrations from 1 wt % to 8 wt %.

To further investigate EL property of the $Eu_2(DBM)_6(FPhOXD6CzPhen_2)$-doped devices, we measured the EL spectra of the device at 2 wt % dopant concentration under different applied voltages, which is shown in Fig. 6. The EL spectra exhibit little change at the given applied voltages, which contain a sharp red emission at 614 nm with a full width at half maximum (FWHM) of 8 nm. The corresponding CIE coordinates also present a minor change from (0.56, 0.32) to (0.53, 0.34) with increasing driving voltages from 10 V to 16 V, as shown in Fig. 6 (inset). This means that stable red emissions were obtained in the $Eu_2(DBM)_6(FPhOXD6CzPhen_2)$-doped devices at 2 wt % dopant concentration under different bias.

Fig. 7 exhibits the current density-voltage-brightness (*J-V-B*) curves of the $Eu_2(DBM)_6(FPhOXD6CzPhen_2)$-doped devices at different doping concentrations from 1 wt % to 8 wt %. The maximum brightness of 48.5 cd/m^2 was obtained in the device at

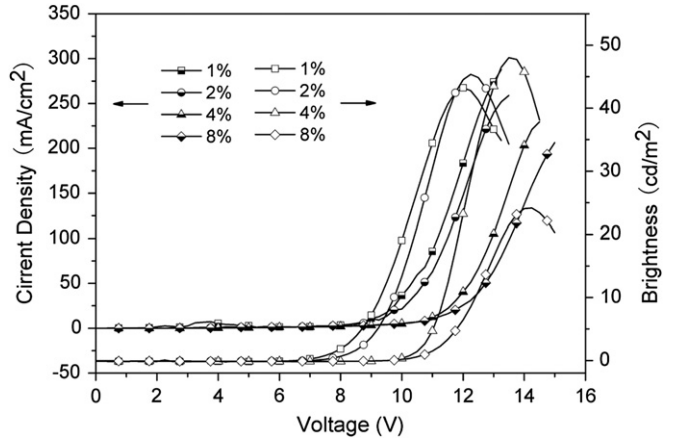

Fig. 7. The current density-voltage-brightness (*J-V-B*) characteristics of the $Eu_2(DBM)_6(FPhOXD6CzPhen_2)$-doped PVK-PBD devices with different dopant concentrations from 1 wt % to 8 wt %.

4 wt % dopant concentration under a driving voltage of 13.5 V. Compared to the unfunctionlized dinuclear europium complex of $Eu_2(dbm)_6(bpm)$, this bipolar-transporting dinuclear europium complex of $Eu_2(DBM)_6(FPhOXD6CzPhen_2)$ exhibited a higher brightness in the PLEDs with the same device structure. The results further indicate that an introduction of bipolar-transporting groups into neutral ligand can improve the performance of its europium (III) complex-doped PLEDs.

4. Conclusion

In summary, a series of bipolar-transporting dinuclear europium complexes of $Eu_2(DBM)_6(RPhOXD6CzPhen_2)$ with both carbazole and oxadiazole units were obtained. These dinuclear europium complexes presented higher thermal stability, more intense UV-vis absorption at high-energy area as well as higher emission quantum yield in DCM solution. Compared to the reported the mononuclear $Eu(DBM)_3Phen$, a red sharp emission at 614 nm was obtained for the $Eu_2(DBM)_6(FPhOXD6CzPhen_2)$-doped PVK devices at different dopant concentrations and applied voltages. The results demonstrate that incorporation of a bipolar-transporting moiety into the europium (III) complex can improves the performance of the PLEDs.

Acknowledgments

The authors thank the National Natural Science Foundation of China (Project No.20872124, 50973053 and 21172187), the Specialized Research Fund and New Teacher Fund for the Doctoral Program of Higher Education (20094301110004, 200805301013), the Open Project Program of Key Laboratory of Environmentally Friendly Chemistry and Applications of Ministry of Education (09HJYH06), the Scientific Research Fund of Hunan Provincial Education Department (11CY023, 10A119, 10B112), the Hunan Provincial Natural Science Foundation of China (11JJ3061), the Postgraduate Science Foundation for Innovation in Hunan Province (CX2011263) and Hunan Undergraduate Investigated-Study and Innovated-Experiment Plan for the financial support of this research.

References

[1] Crosby G-A, Whan R-E, Alire R-M. Intramolecular energy transfer in rare earth chelates. Role of the triplet state. J Chem Phys 1961;34:743–8.
[2] Kido J, Nagai K, Okamoto Y, Skotheim T. Electroluminescence from polysilane film doped with europium complex. Chem Lett; 1991:1267–9.
[3] Gao X-C, Cao H, Huang C-H, Li B-G, Umitani S. Electroluminescence of a novel terbium complex. Appl Phys Lett 1998;72:2217–9.
[4] Baldo M-A, Adachi C, Forrest S-R. Transient analysis of organic electrophosphorescence.II. Transient analysis of triplet-triplet annihilation. Phys Rev B 2001;62:10967–77.
[5] Sun P-P, Duan J-P, Shih H-T, Cheng C-H. Europium complex as a highly efficient red emitter in electroluminescent devices. Appl Phys Lett 2002;81:792–4.
[6] Fang J-F, You H, Gao J, Ma D-G. Improved efficiency by a fluorescent dye in red organic light-emitting devices based on a europium complex. Chem Phys Lett 2004;392:11–6.
[7] Robinson M-R, Ostrowski J-C, Bazan G-C, McGehee M-D. Reduced operating voltages in polymer light-emitting diodes doped with rare-earth complex. Adv Mate 2003;15:1547–51.
[8] Canzler T-W, Kido J. Exciton quenching in highly efficient europium complex based organic light-emitting diodes. Org Electron 2006;7:29–37.
[9] Zhou L, Zhang H-J, Shi W-D, Deng R-P, Li Z-F, Yu J-B, et al. Mechanisms of efficiency enhancement in the doped electroluminescent devices based on a europium complex. J.Appl Phys 2008;104:114507–114511-7.
[10] Xu H, Yin K, Huang W. Novel light-emitting ternary Eu^{3+} complexes based on multifunctional bidentate aryl phosphine oxide derivatives: tuning photophysical and electrochemical properties toward bright electroluminescence. J Phys Chem C 2010;114:1674–83.
[11] Li X, Xiao G-Y, Chi H-J, Dong Y, Zhao H-B, Lei P, et al. A novel fluorinated europium ternary complex for highly efficient pure red electroluminescence. Mater Chem Phys 2010;123:289–92.

[12] McGehee M-D, Bergstedt T, Zhang C, Saab A-P, O'Regan M-B, Bazan G-C, et al. Narrow bandwidth luminescence from blends with energy transfer from semiconducting conjugated polymers to europium complexes. Adv Mater 1999;11:1349–54.
[13] Peng J-B, Takada N, Minami N. Red electroluminescence of a europium complex dispersed in poly(N-vinylcarbazole). Thin Solid Films 2002;405:224–7.
[14] O'Riordan A, O'Connor E, Moynihan S, Llinares X, Deun R-V, Fias P, et al. Narrow bandwidth red electroluminescence from solution- processed lanthanide-doped polymer thin films. Thin Solid Films 2005;49:264–9.
[15] Liu Y, Li J-D, Li C, Song J-G, Zhang Y-L, Peng J-B, et al. Highly efficient sharp red electroluminescence from europium complex-doped poly(9,9-dioctylfluorene) devices. Chem Phys Lett 2007;433:331–4.
[16] Giovanella U, Pasini M, Freund C, Botta C, Porzio W, Destri S. Highly efficient color-tunable OLED based on poly(9,9-dioctylfluorene) doped with a novel europium complex. J Phys Chem C 2009;113:2290–5.
[17] Jiang X, Jen A-K-Y, Phelan G-D, Huang D, Londergan T-M, Dalton L-R, et al. Efficient emission from a europium complex containing dendron-substituted diketone ligands. Thin Solid Films 2002;416:212–7.
[18] Xiang N-J, Leung L-M, So S-K, Wang J, Su Q, Gong M-L. Red InGaN-based light-emitting diodes with a novel europium (III) tetrabasic complex as mono-phosphor. Mater Lett 2006;60:2909–13.
[19] Li S-f, Zhu W-H, Xu Z-Y, Pan J-F, Tian H. Antenna-functionalized dendritic b-diketonates and europium complexes: synthetic approaches to generation growth. Tetrahedron 2006;62:5035–48.
[20] Zheng Y-X, Cardinali F, Armaroli N, Accorsi G. Synthesis and photo-luminescence properties of heteroleptic europium (III) complexes with appended carbazole units. Eur J Inorg Chem; 2008:2075–80.
[21] Sun M, Xin H, Wang K-Z, Zhang A-Y, Jin L-P, Huang C-H. Bright and mono-chromic red light-emitting electroluminescence devices based on a new multifunctional europium ternary complex. Chem Commun; 2003:702–3.
[22] Liu Y, Wang Y-F, Guo H-P, Zhu M-X, Li C, Peng J-B. Red-emitting europium(III) complex containing triphenylamine-functionalized phenanthroline. J Phys Chem C 2011;115:4209–16.
[23] Xin H, Li F-Y, Guan M, Huang C-H, Sun M, Wang K-Z, et al. Carbazole- functionalized europium complex and its high-efficiency organic electrolumi-nescent properties. J Appl Phys 2003;94:4729–31.
[24] Guan M, Bian Z-Q, Li F-Y, Xin H, Huang C-H. Bright red light-emitting elec-troluminescence devices based on a functionalized europium complex. New J Chem 2003;27:1731–4.
[25] Xin H, Sun M, Wang K-Z, Zhang Y-A, Jin L-P, Huang C-H. Voltage-independent pure red devices based on a carbazole-functionalized europium complex. Chem Phys Lett 2004;388:55–7.
[26] Zhang L-Y, Li T-L, Li B, Lei B-F, Yue S-M, Li W-L. Synthesis and electrolumi-nescent properties of a carbazole-functionalized europium(III) complex. J Lumin 2007;126:682–6.
[27] Wu J, Li H-Y, Xu Q-L, Zhu Y-C, Tao Y-M, Li H-R, et al. Synthesis and photo-luminescent properties of series ternary lanthanide (Eu(III), Sm(III), Nd(III), Er(III), Yb(III)) complexes containing 4,4,4-trifluoro-1-(2-naphthyl)-1,3-butanedionate and carbazole-functionalized ligand. Inorg Chim Acta 2010; 363:2394–400.
[28] Liang F-S, Zhou Q-G, Cheng Y-X, Wang L-X, Ma D-G, Jing B, et al. Oxadiazole-functionalized europium(III) β-diketonate complex for efficient red electro-luminescence. Chem Mater 2003;15:1935–7.
[29] Liu Z, Wen F-S, Li W-L. Synthesis and electroluminescence properties of europium (III) complexes with new second ligands. Thin Solid Films 2005; 478:265–70.
[30] Tang R-R, Zhang W, Luo Y-M, Li J. Synthesis, fluorescence properties of Eu(III) complexes with novel carbazole functionalized β-diketone ligand. J Rare Earths 2009;27:362–7.
[31] Tang H-J, Tang H, Zhang Z-G, Yuan J-B, Cong C-J, Zhang K-L. Synthesis, pho-toluminescent and electroluminescent properties of a novel europium(III) complex involving both hole- and electron-transporting functional groups. Synth Met 2009;159:72–7.
[32] Li L, Liu Y, Guo H-P, Wang Y-F, Cao Y-B, Liang A-H, et al. Synthesis, opto-physical and electrochemical properties of bipolar-transporting europium(III) complexes with carbazole and oxadiazole units. Tetrahedron 2010;66: 7411–7.
[33] Bassett A-P, Magennis S-W, Glover P-B, Lewis D-J, Spencer N, Parsons S, et al. Highly Luminescent, triple- and quadruple-stranded, dinuclear Eu, Nd, and Sm(III) lanthanide complexes based on bis-diketonate ligands. J Am Chem Soc 2004;126:9413–24.
[34] You H, Fang J-F, Wang L-H, Zhu X-H, Huang W, Ma D-G. Efficient red organic light- emitting diodes based on a dinuclear europium complex. Opt Mater 2007;29:1514–7.
[35] He P, Wang H-H, Liu S-G, Shi J-X, Wang G, Gong M-L. Visible-light excitable europium(III) complexes with 2,7-positional substituted carbazole group-containing ligands. Inorg Chem 2009;48:11382–7.
[36] Liu S-G, He P, Wang H-H, Shi J-X, Gong M-L. A highly luminescent dinuclear Eu(III) complex based on 4,4'-bis (4",4",4"-trifluoro-1",3"-dioxobutyl)-o-terphenyl for light- emitting diodes. Mater Chem Phys 2009;116:654–7.
[37] Liu S-G, He P, Wan H-H, Shi J-X, Gong M-L. A luminescent dinuclear Eu(III) complex based on 2,8-bis(4',4',4',-trifluoro-1',3'-dioxobutyl)-dibenzothio-phene for light-emitting diodes. J Lumin 2010;130:855–8.
[38] Jang H, Shin C-H, Jung B-G, Kim D-H, Shim H-K, Do Y-K. Synthesis and characterization of dinuclear europium complexes showing pure red elec-troluminescence. Eur J Inorg Chem; 2006:718–25.
[39] Liu Y, Su GJ, Xing K-Q, Gan Q, Yang Y-P, Zhu W-G. Synthesis of 2-aryl-5-(4-bromopheny1)-1,3,4-oxadiazole derivatives and studies on their spectral properties. Nat Sci J Xiangtan Univ 2006;28:68–71 [in Chinese].
[40] Xu Z-W, Li Y, Ma X-M, Gao X-D, Tian H. Synthesis and properties of iridium complexes based 1,3,4-oxadiazoles derivatives. Tetrahedron 2008;64: 1860–7.
[41] Lecomte J-P, Mesmaeker A-K-D, Lhomme J. Synthesis and characterisation of a new DNA-binding bifunctional ruthenium(II) complex. J Chem Soc Faraday Trans 1993;89:3261–9.
[42] Ueno K, Martell A-E. Infrared studies on synthetic oxygen carriers. J Phys Chem 1956;60:1270–5.
[43] Xu C-J, Li B-G, Wan J-T, Bu Z-Y. Synthesis and characterization of a Eu-containing polymer precursor featuring thenoyltrifluoroacetone and 5-acrylamido-1,10-phenanthroline. Spectrochim Acta A 2011;82:159–63.
[44] Bian Z-Q, Gao D-Q, Guang M, Xin H, Li F-Y, Wang K-Z, et al. Study on the electroluminescent properties of ternary Europium complexes with different phenanthroline derivatives as neutral ligands. Sci China B Chem 2004;34: 113–20 [in Chinese].
[45] Zhang Y, Shi H-H, Ke Y, Cao Y. Synthesis and characterization of highly fluo-rescent europium functionalized β-diketonate complexes. J Lumin 2007;124: 51–7.
[46] Bredas J-L, Silbey R, Boudreaux D-S, Chance R-R. Chain-length dependence of electronic and electrochemical properties of conjugated systems: poly-acetylene, polyphenylene, polythiophene, and polypyrrole. J Am Chem Soc 1983;105:6555–9.